Silicon Nanotube Battery Anodes

Mi-Hee Park,[†] Min Gyu Kim,[‡] Jaebum Joo,[§] Kitae Kim,[||] Jeyoung Kim,[||] Soonho Ahn,[||] Yi Cui,[*,⊥] and Jaephil Cho[*,†]

School of Energy Engineering, Ulsan National Institute of Science & Technology, Ulsan, Korea 689-798, Beamline Research Division, Pohang Accelerator Laboratory, Pohang, Korea 790-784, Department of Applied Chemistry, Hanyang University, Ansan, Korea 426-791, Battery R&D, LG Chem, Ltd. 104-1, Moonji-dong, Yuseong-gu, Daejeon, Korea 305-380, and Department of Materials Science and Engineering, Stanford University, Stanford, California 94305

ABSTRACT

We present Si nanotubes prepared by reductive decomposition of a silicon precursor in an alumina template and etching. These nanotubes show impressive results, which shows very high reversible charge capacity of 3247 mA h/g with Coulombic efficiency of 89%, and also demonstrate superior capacity retention even at 5C rate (=15 A/g). Furthermore, the capacity in a Li-ion full cell consisting of a cathode of $LiCoO_2$ and anode of Si nanotubes demonstrates a 10 times higher capacity than commercially available graphite even after 200 cycles.

The specific energy storage capacity and the charge/discharge rate of lithium ion batteries are critical for their use in electric vehicles (EVs) and to store energy produced by intermittent sources such as solar cells and wind.[1] Despite significant gains in rate capability and safety through the use of new materials,[2,3] increasing specific energy capacity remains a challenge. Replacing graphitic carbon with Si as the anode material can result in an increase in anode capacity by a factor of 10 and can considerably increase the energy capacity of the total battery. However, a rapid loss of the reversible capacity upon cycling, which is associated with the large volume expansion of Si, is a challenge.[4] Recent studies on Si nanowires[5,6] and nanoporous Si[7] show great promise in overcoming this issue.

When reacting with Li, Si is known to incorporate 4.4 Li atoms per Si atom. In Li-ion batteries, this results in the extremely high specific capacity of 4200 mA h/g, which is 10 times higher than the capacity of graphitic carbon (372 mA h/g).[8,9] However, the 300% volume change upon lithium insertion commonly causes pulverization and thus a loss of electrical contact between Si and the current collector. Previous studies on improving the capacity of Si-based materials have been focused on nanoparticle composites and carbon prepared by ball-milling and thermal reduction.[10−17] Despite these efforts, these electrodes still suffer from rapid

capacity fading. Recently, Si nanowires[5,6] and 3D porous Si particles[18] have been demonstrated to exhibit good cycling performance as anode materials since both types of structures provide empty space to accommodate Si volume changes and allow for facile strain relaxation without mechanical fracture upon lithium insertion. However, these materials exhibited increased polarization at higher current rates and some degree of capacity fading over many cycles, which could possibly be due to the limited surface area accessible to the electrolyte and the continuous growth of solid electrolyte interphase (SEI) at the interface between the silicon and electrolyte. For instance, hollow nestlike silicon nanospheres showed the first discharge capacity (lithium dealloy) of 3052 mA h/g at a rate of 2000 mA/g, but its Coulombic efficiency and capacity retention ratio after 50 cycles were 73% and <25% (~1000 mA h/g), respectively.[14]

Here, we fabricate novel Si nanotube structures and demonstrate their superior cycling performance for the first time. The nanotube electrodes have ultrahigh reversible charge capacities of ~3200 mA h/g and have outstanding capacity retention of 89% after 200 cycles at a rate of 1C in practical Li-ion cells.

In this work, we used Si nanotubes (Figure 1) to increase the surface area accessible to the electrolyte, which allows the Li ions to intercalate at the interior and exterior of the nanotubes. In addition, we deposited a carbon coating on the surface of the nanotubes, which stabilizes the Si–electrolyte interface and promotes stable SEI formation for long cycle life. To synthesize carbon-coated Si nanotubes, a method involving chemical deposition within porous alumina membrane templates was employed. (See Supporting Information

---

* Corresponding authors, jpcho@unist.ac.kr and yicui@stanford.edu.
† School of Energy Engineering, Ulsan National Institute of Science & Technology.
‡ Beamline Research Division, Pohang Accelerator Laboratory.
§ Department of Applied Chemistry, Hanyang University.
|| Battery R&D, LG Chem, Ltd.
⊥ Department of Materials Science and Engineering, Stanford University.
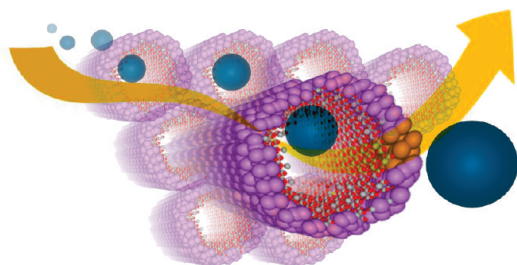
Figure 1. Schematic diagram of Li-ion pathway in Si nanotubes.
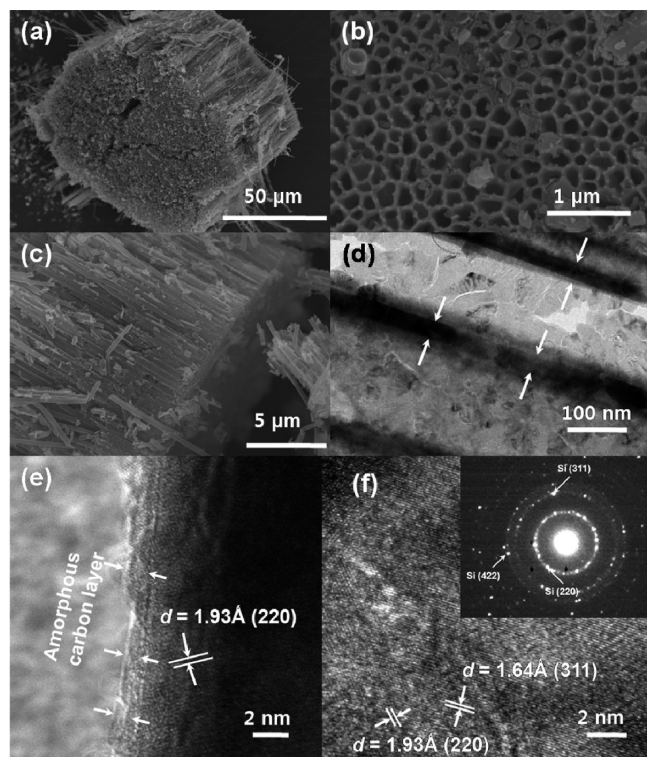
Figure 2. (a, b, and c) FE-SEM images of Si nanotubes: (b) top view and (c) side view. (d, e, and f) TEM images of Si nanotubes: (e) edge of the outer wall and (f) inner surface of nanotube wall. The inserted figure in (f) is a selected area diffraction pattern of (f). Arrows in image d indicate the tubewalls.

for detailed synthesis procedures.)

Figure 2 shows scanning electron microscopy (SEM) (Figure 2a−c) and transmission electron microscopy (TEM) (Figure 2d) images of the Si nanotubes after the removal of the alumina template by treatment with NaOH (also see Figure S1 in Supporting Information). The carbon coating protects the Si nanotubes from being etched away by NaOH. The assemblies of uniform Si nanotubes with outer diameters of ∼200−250 nm were recovered, and their wall thickness was measured to be ∼40 nm as indicated by arrows. After ultrasonication, the Si nanotube bundles were separated (see Figure S2 in Supporting Information). The side view of the bundle of nanotubes in Figure 2a shows a tube length of ∼40 μm and the top-view SEM image in Figure 2b shows the open ends of the nanotubes. Figure 2e shows a high-resolution TEM (HRTEM) image of the surface of the outer wall of a nanotube, which indicates that the outermost layer is covered with nanometer thick amorphous carbon, although
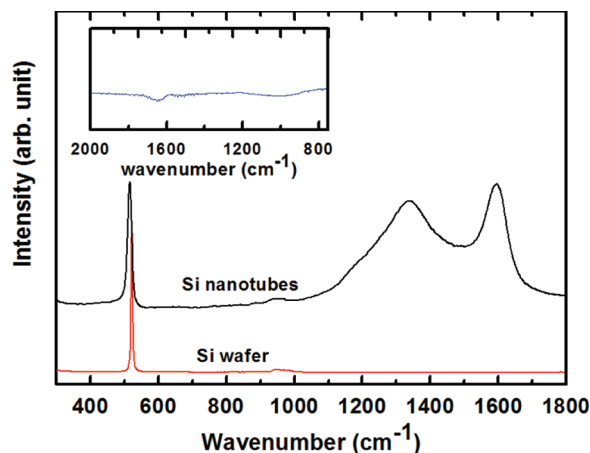
Figure 3. Raman spectra of Si nanotubes and Si wafer reference. The insert is a FT-IR spectrum of Si nanotubes.

weak lattice fringes with a d spacing of 1.93 Å can also be observed, corresponding to the Si(220) plane. Figure 2f is an HRTEM image of the inner surface of a nanotube wall, and selected area diffraction pattern and lattice fringe images confirm the dominant presence of a crystalline Si phase although we cannot rule out possible presence of minor amorphous Si phase. The X-ray diffraction (XRD) pattern of the Si nanotubes shows the presence of the diamond cubic Si phase (Figure S3 in Supporting Information) and crystallite size was estimated to ∼10 nm.

Figure 3 shows the Raman spectrum of the Si nanotubes. The sharp peak at ∼516 cm^{-1} is related to the Si−Si stretching mode, which is identical to that of the reference Si wafer. A small peak at ∼957 cm^{-1} is due to the stretching mode of amorphous Si−Si, which is also observed in the Si wafer. The two other peaks at ∼1360 and ∼1580 cm^{-1} are assigned to the D band (disordered band) and G band (graphene band) of carbon, respectively.[19] These peaks confirm the carbon coating on the surface of the Si nanotubes; the carbon is deposited by the high-temperature decomposition of the organic precursors used for the synthesis of the Si nanotubes. The dimensional ratio of the D and G bands of the samples can be estimated to be 1.4. This value is much smaller than the values previously reported for carbon-coated Si nanoparticles[20] and Sn$_{0.9}$Si$_{0.1}$ nanoparticles,[21] which have a ratio larger than 2. We do not observe a peak in the range of 1000−1100 cm^{-1} for SiO$_2$ using FT-IR spectrometry (Figure 3 inset), suggesting that there is little SiO$_2$ on the Si nanotube surface. Therefore, the prepared Si nanotubes can be considered to be at least as pure as the detection limit (100 ppm) of FT-IR. Overall, these results indicate that the Si nanotubes are coated with a very thin layer of amorphous carbon.

Parts a and b of Figure 4 show electrochemical rate capability and cycle life performance of the Si nanotubes in coin-type half cells. The first discharge and charge capacities of the Si nanotubes are 3648 and 3247 mA h/g at the 0.2C rate, respectively, which demonstrates an excellent Coulombic efficiency of 89%. The high value of the Coulombic efficiency of the first cycle is believed to be due to the thin carbon layer, which minimizes the direct contact between
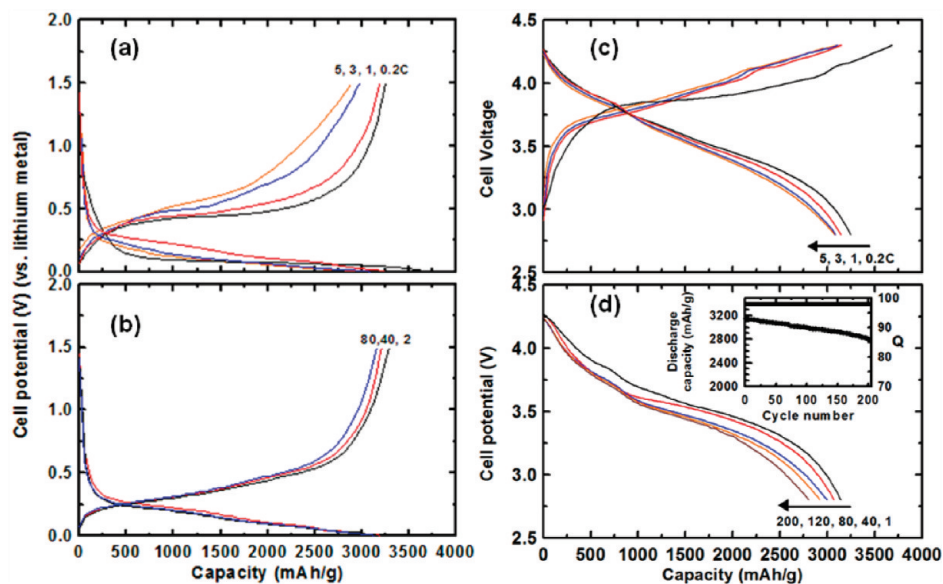
Figure 4. (a and b) Rate capability and voltage profiles of the Si nanotubes in coin-type half cells (vs lithium metal) between 0 and 1.5 V. Cells for (a) used a fixed 1C rate during all the discharge cycles and were tested with increasing rates from 0.2C to 5C (=15 A/g) during the charge cycles. Cells for (b) were cycled at a rate of 1C between 0 and 1.5 V and voltage profiles were plotted after the 2nd, 40th, and 80th cycles. (c and d) Rate capability and cycle life performance of the Si nanotubes in pouch-type Li-ion cells (cathode was LiCoO$_2$) between 2.75 and 4.3 V to 200 cycles. Rate was increased from 0.2C to 5C with the same rates during charge and discharge (1C = 3 A/g). C rate for the cycle test in (d) was 1C.
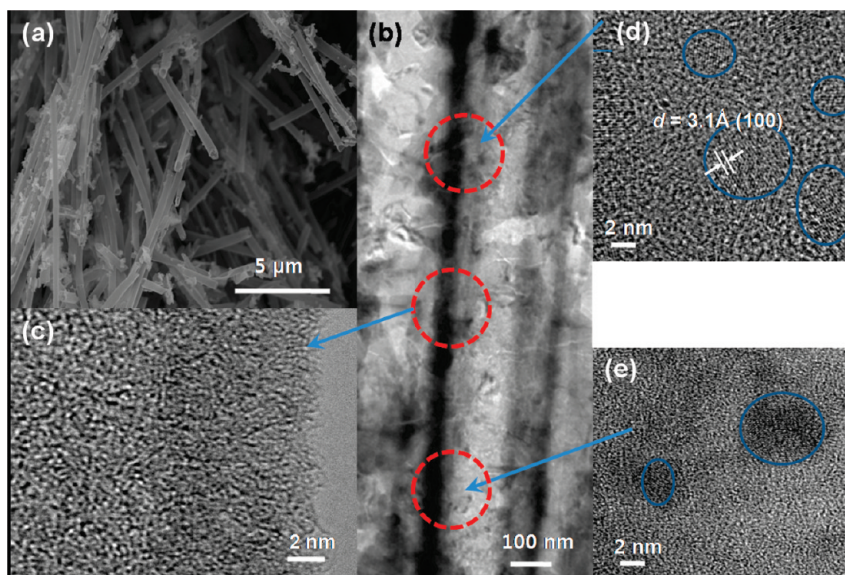
Figure 5. (a) SEM image of cycled Si nanotubes (Si nanotubes were extracted from the Li-ion cell after 200 cycles). (b) TEM image of (a). (c, d, and e) HREM images of dotted red circles in (b). Blue circles indicate the nanocrystalline domains.

the Si and electrolyte and promotes the formation of a stable SEI layer on the inner and outer surface of the Si nanotubes. It has been reported that bare Si particles undergoing Li alloying and dealloying reactions are continually exposed to the electrolyte due to the recurrent generation of new active surfaces that were previously passivated by stable surface films, accelerating capacity fade.[22,23] Coating methods decrease the capacity fade of these particles. For instance, an AlPO$_4$ coating on SnO$_2$ bulk particles was shown to diminish the repetitive formation of electrode/electrolyte interfaces.[23] In the present work, the charge capacity of Si nanotubes at a 5C rate is 2878 mA h/g, representing a higher value than

all previous studies at such a fast rate. Rate capability and cycle life to 200 cycles were also tested by using a Li-ion full cell consisting of a LiCoO$_2$-based cathode and a Si-nanotube-based anode (Figure 4, parts c and d). Excitingly, the initial capacity at rates of both 3C and 5C is above 3000 mA h/g, and capacity retention after 200 cycles is 89% at a rate of 1C. These results are quite comparable to a cell made with commercial graphite.

In order to determine whether the Si nanotube morphology is changed after 200 cycles, the cells were disassembled and the anode was further characterized. Figure 5a shows an SEM image of the electrode after 200 cycles; its original morphol-

ogy is apparently retained. Panels c, d, and e of Figure 5 show HRTEM images of different portions of the single nanotube shown in Figure 5b. These images show that the amorphous phase of Si is dominant, which agrees with previous observations of structural changes in Si after reaction with Li.[24,25] In general, amorphization occurs when a thermodynamically preferred crystalline intermediate compound is unable to nucleate and an amorphous phase that is metastable yet lower in free energy than the pure reactants forms instead.[26] In addition to the amorphous phase, panels c−e of Figure 5 also show the presence of crystalline Si regions less than 5 nm in thickness surrounded by the amorphous matrix. The possible retention or formation of Si nanocrystals has previously been observed in Si anodes after 80 cycles.[18] In this previous work, the XRD pattern of the Si electrode (after charging to 1.5 V) suggested that the Si was fully amorphous, while the HRTEM revealed the presence of Si nanocrystals with sizes smaller than 5 nm. In nanomaterials, the energy barrier for nucleation should be smaller because a large fraction of the Si atoms is in high energy states at the highly metastable surfaces.[27] Due to its highly disordered nature, the amorphous Si matrix has many defects, which could act as preferred nucleation sites for the formation of Si nanoclusters after long-term cycling.

In addition to these structural changes, Figure 5a shows that the morphology of the nanotubes did not change after cycling. The initial pore wall thickness of the Si nanotubes is ∼40 nm, and no pulverization occurred even though the thickness expanded to ∼300 nm. This result supports previous findings that show increased fracture toughness of lithiated silicon nanoparticles with sizes smaller than 20 nm[28] and improved mechanical properties in nanowires with diameters less than 100 nm.[29,30] This effect could be because the surface area to volume ratio increases dramatically when size decreases to the nanometer range, and any dislocations may be quickly drawn to the surface.[28,29]

In conclusion, Si nanotubes were prepared by reductive decomposition of a silicon precursor in the alumina template and etching. These nanotubes showed impressive results, which had very high reversible charge capacity of 3247 mA h/g with Coulombic efficiency of 89% and also demonstrated superior capacity retention even at a 5C rate (=15A/g). Furthermore, the capacity in Li-ion full cell consisting of cathode $LiCoO_2$ and anode Si nanotube demonstrated 10 times higher capacity than commercially available graphite even after 200 cycles.

Supporting Information Available: Experimental details, TEM and SEM images, and XRD pattern of Si nanotubes. This material is available free of charge via the Internet at http://pubs.acs.org.

References

(1) Nazari, G.-A.; Pistoia, G. *Lithium Batteries: Science and Technology*; Kluwer Academic/Plenum: Boston, 2004.
(2) Kang, B.; Ceder, G. *Nature* **2009**, *458*, 190.
(3) Nam, K. T.; Kim, D. W.; Yoo, P. J.; Chiang, C. Y.; Meethong, N.; Hammond, P. T.; Chiang, Y. -M.; Belcher, A. M *Science* **2006**, *312*, 885.
(4) Kasavajjula, U.; Wang, C.; Appleby, A. J. *J. Power Sources* **2007**, *163*, 1003.
(5) Chan, C. K.; Cui, Y. *Nat. Nanotechnol.* **2008**, *3*, 31.
(6) Cui, L. Y.; Cui, Y. *Nano Lett.* **2009**, *9*, 191.
(7) Kim, H.; Cho, J. *Nano Lett.* **2008**, *8*, 3688.
(8) Wakihara, M., Yamamoto, O. *Lithium Batteries-Fundamentals and Performance*; Wiley-VCH: Germany, 1998.
(9) Boukamp, B. A.; Lesh, G. C.; Huggins, R. A. *J. Electrochem. Soc.* **1981**, *128*, 725.
(10) Wang, G. X.; Yao, J.; Liu, H. K. *J. Electrochem. Soc.* **2004**, *7*, A250.
(11) Wang, C. S.; Wu, G. T.; Zhang, X. B.; Qi, Z. F.; Li, W. Z. *J. Electrochem. Soc.* **1998**, *145*, 2751.
(12) Yang, J.; Wang, B. F.; Wang, K.; Liu, Y.; Xie, J. Y.; Wen, Z. S. *Electrochem. Solid-State Lett.* **2003**, *6*, A154.
(13) Holzapfel, M.; Buqa, H.; Scheifele, W.; Novak, P.; Petrat, F. -M. *Chem. Commun.* **2005**, 1566.
(14) Ma, H.; Cheng, F.; Chen, J.; Zhao, J.; Li, C.; Tao, Z.; Liang, J. *Adv. Mater.* **2007**, *19*, 4067.
(15) Hu, Y. -S.; Demir-Cakan, R.; Titirici, M.-M.; Müller, J.-O.; Maier, J. *Angew. Chem., Int. Ed* **2008**, *47*, 1645.
(16) Dimov, N.; Kugino, S.; Yoshio, M. *J. Power Sources* **2004**, *136*, 108.
(17) Lee, H.; Kim, H.; Doo, S.-G.; Cho, J. *J. Electrochem. Soc.* **2007**, *154*, A343.
(18) Kim, H.; Han, B.; Choo, J.; Cho, J. *Angew. Chem., Int. Ed.* **2008**, *47*, 10151.
(19) Tuinstra, F.; Koenig, J. L. *J. Chem. Phys.* **1970**, *53*, 1126.
(20) Kwon, Y. G.; Park, K.-S.; Cho, J. *Electrochim. Acta* **2007**, *52*, 4663.
(21) Kwon, Y.; Kim, H.; Doo, S.-G.; Cho, J. *Chem. Mater.* **2007**, *19*, 982.
(22) Chan, C. K.; Ruffo, R.; Hong, S. S; Cui, Y. *J. Power Sources* **2009**, *189*, 1132.
(23) Kim, T.-J.; Son, S.; Park, B.; Cho, J. *Electrochim. Acta* **2004**, *49*, 4405.
(24) Li, J.; Dahn, J. R. *J. Electrochem. Soc.* **2007**, *154*, A156.
(25) Obrovac, M. N.; Christensen, L. *Electrochem. Soild-State Lett.* **2004**, *7*, A93.
(26) Limthongkul, P.; Jang, Y.-I.; Dudney, N. J.; Chiang, Y.-M. *Acta Mater.* **2003**, *51*, 1103.
(27) Cao, G. *Nanostructures & Nanomaterials*; Imperial College Press: Singapore, 2004.
(28) Graetz, J.; Ahn, C. C.; Yazami, R.; Fultz, B. *Electrochem. Soild-State Lett.* **2003**, *6*, A194.
(29) Gordon, M. J.; Baron, T.; Dhalluin, F.; Gentile, P.; Ferret, P. *Nano Lett.* **2009**, *9*, 525.
(30) McDowell, M. T.; Leach, A. M.; Gall, K. *Nano Lett.* **2008**, *8*, 3613.
(31) Baldwin, B. K.; Pettigrew, K. A.; Carno, J. C.; Power, P. P.; Liu, G.; Kauzlarich, S. M. *J. Am. Chem. Soc.* **2002**, *124*, 1150.
(32) Baldwin, B. K.; Katherine, A.; Pettigrew, A.; Augustine, E. M. P.; Kauzlarich, S. M. *Chem. Commun.* **2002**, 1822.

NL902058C